

Effect of Temperature on the Properties of Charcoal Prepared from Carbonization of Biorefinery Lignin

Xiao-Fei Wu,^a Shu-Xian Li,^a and Ming-Fei Li^{a,b,*}

Biorefinery lignin was carbonized under a carbon dioxide atmosphere at various temperatures *viz.*, 500 °C, 600 °C, 700 °C, and 800 °C, separately. The results indicated that with increasing temperature, the mass yield decreased from 49.2% to 39.8%. Carbonization at a high temperature resulted in an increment of carbon (C) content and decreased both the hydrogen (H) and oxygen (O) contents. With the increase of carbonization severity, the ratios of O/C and H/C decreased mainly due to the demethanation, dehydration, and decarboxylation reactions. The carbonization resulted in the transformation of aromatic rings as well as the rearrangement of the aromatic polymers, and the enhancement of the thermal stability of the charcoal formed.

Keywords: Biorefinery lignin; Carbonization; Charcoal; Structural change

Contact information: a: Beijing Key Laboratory of Lignocellulosic Chemistry, Beijing Forestry University, Beijing 100083, China; and b: Jiangsu Ginaton Biotechnology Co., Ltd., Xuzhou, Jiangsu 276127, China;
* Corresponding author: limingfei@bjfu.edu.cn

INTRODUCTION

Currently, society relies heavily on coal, petroleum, and natural gas. However, the limited nature of these nonrenewable resources, coupled with related environmental problems, make it imperative to find new alternate solutions to replace them. Lignin, a biopolymer obtained from renewable sources, is the third most abundant material in the terrestrial region after cellulose and hemicelluloses. It is an amorphous phenolic polymer consisting of different ratios of *p*-coumaryl, coniferyl, and sinapyl alcohol monomers. Different linkages, such as β -O-4, β - β , β -5, β -1, 5-5, and 4-O-5 bonds, connect these monomers. Traditionally, lignin is mainly obtained from lignocellulosic biomass in the forms of kraft lignin, soda lignin, and lignosulfonates. Recently, the development of the biorefinery industry is resulting in the production of a sustainable supply of lignin and also stimulates the transformation of this cheap resource into value-added products widely used in the fields of energy and materials (Ma *et al.* 2014; Dávila *et al.* 2017).

The thermochemical conversion of lignin is considered a promising way to volatilize lignin for the preparation of multiple energy-rich material products. The thermochemical conversion process, including liquefaction, carbonization, pyrolysis, gasification, *etc.*, involves several chemical reactions and is mainly affected by the nature of the raw material, reaction temperature, heating rate, and reaction time (Pandey and Kim 2011; Hu *et al.* 2013; Mudraboyina *et al.* 2016). It has been revealed that the lignin without or with lower sulfur content has wider applications because it can reduce the toxic gas emission problems during the processing and disposal stages (Sahoo *et al.* 2011). In the last decade, there have been many studies on the gas and tar products formed from lignin, while little attention has been paid to charcoal.

Electromagnetic shielding material was prepared by carbonization of a mixture of wood and nickel at a high temperature, which suggested charcoal is a promising material for substitution of metals to manufacture electromagnetic shielding materials (Suzuki *et al.* 2001). The charcoal prepared from lignin showed high specific surface area comparable to commercial active carbon products (Savova *et al.* 2001; Suhas *et al.* 2007). After thermochemical conversion, the prepared functional materials displayed wide applications in the fields of catalyst support (Ronsse *et al.* 2015), as plates for fuel cells (Zhao and Zhu 2016), a candidate for carbon fiber (Souto *et al.* 2015), and in pollutant removal (Liu *et al.* 2015).

With respect to the carbonization of lignocelluloses, most studies have concentrated on the process with respect to the whole wood. During the carbonization of wood, it has been reported that with the increase of temperature from 277 to 877 °C, the yield of charcoal decreased from 42.6% to 30.7% for hazelnut shell, and from 25.6% to 22.7% for beech wood (Demirbas 2009). In addition, the ignition temperature of charcoal increased when the carbonization temperature was elevated. Woods from some tropical trees were carbonized at 400, 600, and 800 °C, and the maximum heating value was obtained after carbonization at 600 °C (Hidayat *et al.* 2017). The carbonization at 600 and 400 °C produced charcoal with the highest energy densification ratio and energy yield, respectively. The influence of final temperature on the properties of charcoal was evaluated during carbonization of babassu nutshell at 450, 550, 650, 750, and 850 °C, and it was found that charcoal and energy yields notably decreased at lower temperatures, but stabilized at higher temperature (Protasio *et al.* 2014). Based on higher heating value, the energy yields were reasonable, and the losses were 45% and 52% when temperature ranged from 450 to 850 °C. For the carbonization of *Paulownia tomentosa* and *Pinus densiflora*, the charcoal obtained showed higher heating value as the carbonization temperature increased. The heating value of the charcoal notably increased from room temperature to 400 °C but increased mildly from 600 to 800 °C (Qi *et al.* 2016). For the carbonization of Sugi wood, it was found that the iodine absorption capacity of the carbonized wood powder was elevated with the increase of carbonization temperature from 400 to 800 °C, but decreased with further increase of temperature (Pulido-Novicio *et al.* 2001).

Although much research has been conducted on the carbonization processes on biomass under nitrogen atmosphere, little attention has been given on the carbonization of lignin under carbon dioxide atmosphere (Pohlmann *et al.* 2014; Ronsse *et al.* 2015; Bilgic *et al.* 2016). Due to the complex structure of lignin, it is imperative to explore the structural properties after the carbonization reaction used for the preparation of charcoal. Therefore, in the present study, a tubal reactor was applied to carbonize a biorefined lignin under carbon dioxide atmosphere at different temperatures, and the charcoals obtained were characterized by elemental analysis, Fourier transform infrared (FTIR) spectroscopy, and thermogravimetric analysis (TGA). The results attained are beneficial for understanding the mechanism of lignin thermal degradation as well as its potential applications.

EXPERIMENTAL

Material

Lignin used in the present study was obtained from a corncob processing biorefinery factory (Shandong Longlive Biotechnology Co., Ltd., Dezhou, China) to prepare the bio-ethanol and chemicals. The sulfur-free biopolymer was first fractionated

from corncob using a diluted NaOH solution, and then precipitated by acid followed by membrane purification. The high purity and sulfur-free lignin thus prepared contained a low amount of carbohydrates (0.6%) and ash (0.5%), and the particle sizes were less than 200 μm .

Methods

Carbonization process

Lignin was carbonized under a carbon dioxide atmosphere in a tubular batch reactor (SK-G08123K; Tianjin Zhonghuan Experimental Furnace Co., Ltd., Tianjin, China). The quartz reactor used had an inner diameter of 92 mm and a length of 1 m that was heated by a furnace with an electrical heater. A total of 10 g of the sample (L0) was placed in a zirconium oxide boat (length 60 mm, width 51 mm, and height 32 mm) and then loaded into the reactor. Next, the reactor was purged with carbon dioxide, and then carbon dioxide with a flow rate of 100 mL/min was supplied. The sample was heated to the target temperature (500 °C, 600 °C, 700 °C, and 800 °C, separately) at 5 °C/min and held at that temperature for 30 min. Then, the heating was stopped and the reactor was cooled to 80 °C. The variation of temperature with time during the whole process was recorded. The carbonized samples were collected and labelled as L500, L600, L700, and L800, respectively.

Characterization of the products

The samples were analyzed using an Elementar Vario EL III elemental analyzer (Elementar Analysensysteme GmbH, Hanau, Germany) to investigate the C, H, and N contents. The O-content was calculated by difference: 100% - (total C, H, and N-contents).

To characterize the structural changes of the specimen, FTIR spectra were collected using a Thermo Scientific Nicolet iN10 FTIR spectrometer (Madison, USA) with a mercury cadmium telluride detector from 650 cm^{-1} to 4000 cm^{-1} at a resolution of 2 cm^{-1} .

Thermogravimetric analysis of the samples was conducted on a TGA analyzer (SDT Q600; TA Instruments, Leatherhead, UK). Approximately 10 mg of the sample was loaded in an aluminum oxide (Al_2O_3) boat and heated from 30 °C to 700 °C at a heating rate of 10 °C/min under nitrogen atmosphere.

Scanning electron microscopy (SEM) images of the samples were recorded on an SEM microscope (S-3400N, HITACHI, Tokyo, Japan) at an acceleration voltage of 10 kV. The bulk density was determined referring to the method reported (Castro *et al.* 2017).

RESULTS AND DISCUSSION

Yield and Elemental Analysis

The mass yield of lignin after carbonization at 500 °C, 600 °C, 700 °C, and 800 °C decreased to 49.2%, 44.9%, 41.3%, and 39.8%, respectively, with increased carbonization temperature. The decrease of the yield was due to the removal of volatile components as well as due to the pyrolysis of lignin under high temperature. This observation was similar to the carbonization of hydrolytic cotton lignin under nitrogen atmosphere, where 65.8% of the raw material was removed after the carbonization at 800 °C (Ismailova 2009).

The elemental composition of the sample is illustrated in Fig. 1. Carbonization at a high temperature increased the C-content and decreased both the H- and O-contents. The C, H, and O contents of the original lignin were 63.2%, 5.9%, and 30.9%, respectively. As the carbonization temperature increased from 500 °C to 800 °C, the C-content progressively increased from 84.2% to 93.8%, while the H- and O-contents decreased from 3.45% to 1.29% and from 13.3% to 4.87%, respectively. The carbonization under carbon dioxide atmosphere produced char with a richer C-content than those obtained from hydrothermal carbonization (Correa *et al.* 2017).

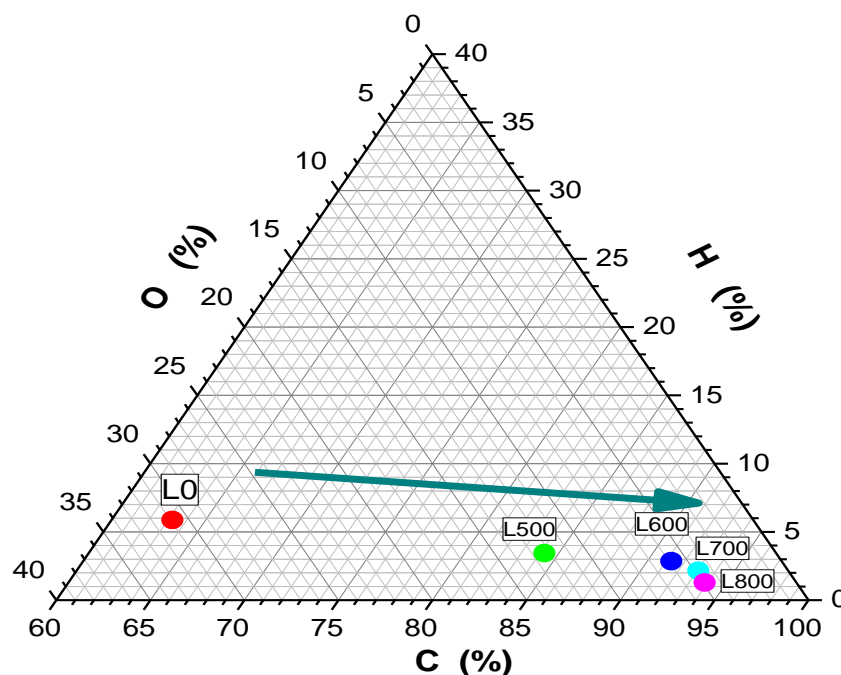


Fig. 1. Ternary diagram for C, H, and O content changes during the carbonization of lignin

The variation of the C, H, and O contents of the products was plotted in a Van Krevelen diagram as shown in Fig. 2. The data change observed was in accordance with a previous report that carbonization of biomass resulted in carbon-rich materials (Wikberg *et al.* 2015). In the carbonization under carbon dioxide process, with the increase of the severity, the gradual decreases of the O- and H- contents were observed, which resulted in the low values of O/C and H/C ratios. As seen in Fig. 2, the data point shifted from the upper right corner to the bottom left corner because the O/C and H/C values showed a reduction trend from L0 to L800. The change of the components was mainly due to the demethanation, dehydration, and decarboxylation reactions. The H/C ratio decreased more drastically than the O/C ratio, signifying that the demethanation and dehydrogenation reactions were the major reactions during the process (Ishimaru *et al.* 2007). The H/C and O/C ratios of the charcoals were notably lower than those of the chars produced from hydrothermal carbonization (H/C and O/C ratios were 0.80 and 0.23 from eucalyptus bark carbonization) (Gao *et al.* 2016) as well as charcoal from low temperature carbonization (H/C and O/C ratios were 0.6 to 1.6 and 0.4 to 0.8 for *Arundo donax* L. and *Phoenix canariensis*) (Correia *et al.* 2017).

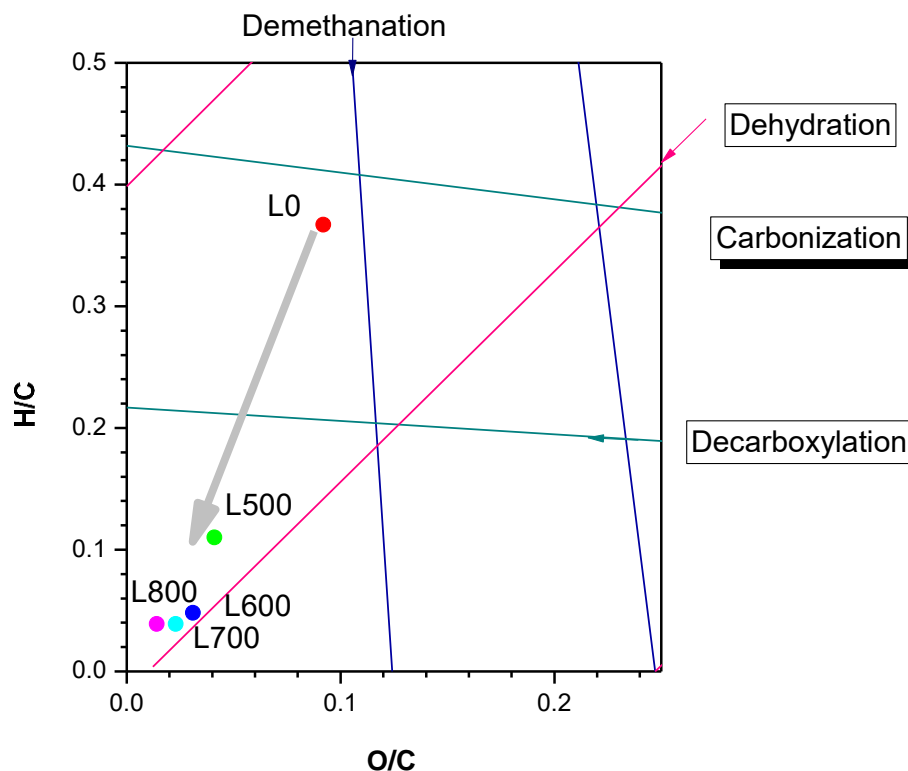


Fig. 2. H/C and O/C ratio variation of the charcoal obtained from carbonization of lignin at various temperatures

FTIR Analysis

To investigate the effect of reaction temperature on the carbonization, FTIR spectra of the solid product obtained were recorded (Fig. 3). The FTIR spectra showed typical signals for the alkaline lignin of corncob. The lignin features were characterized by a broad O-H band at 3397 cm^{-1} , C-H band at 2940 cm^{-1} and 2856 cm^{-1} , carbonyl stretching of conjugated ketonic group at 1687 cm^{-1} , and aromatic skeletal vibrations at 1591 cm^{-1} , 1504 cm^{-1} , and 1421 cm^{-1} . Other signals for typical Gramineae plant lignin were observed at 1455 cm^{-1} (C-H deformation), 1326 cm^{-1} (syringyl (S) ring breathing with C-O stretching), 1118 cm^{-1} (C-H in-plane deformation of secondary alcohol and aliphatic ether, mainly for S-unit), 1028 cm^{-1} (C-H in plane deformation in guaiacyl (G) unit, and C-O deformation of primary alcohol), and 833 cm^{-1} (aromatic C-H out of plane deformation in the position of 2 and 6 of S-unit, and in all positions of *p*-hydroxyphenyl (H) unit). After carbonization, the signals changed drastically. The signals for O-H groups were notably decreased in L500 and disappeared for the samples subjected to higher temperature treatment. The intensities for the C-H band at 2940 cm^{-1} and 2856 cm^{-1} also declined and eventually vanished from the L500 to L800 samples. The intensity of the peak at 1591 cm^{-1} decreased from L0 to L600, and disappeared for the L700 and L800 samples. However, only one major peak for the aromatic group was observed at 1504 cm^{-1} , indicating the transformation to condensed aromatic rings (Cao *et al.* 2013). The increase of the intensity of the signal at 1080 cm^{-1} indicated the enrichment of C-O linkages in the product. Additionally, the signal shifted from 833 cm^{-1} to 866 cm^{-1} in samples L0 to L500 through L800, which indicated the rearrangement of the aromatic polymers. This was also supported by the content of the aforementioned C-element. Overall, an increase in the carbonization temperature increased

the ratio of aromatic carbons to aliphatic carbons, and more condensed aromatic rings were formed. The carbonization under carbon dioxide atmosphere provided a relatively mild condition to prepare charcoal, lower than those at under nitrogen atmosphere (higher than 1200 °C) (Cao *et al.* 2013).

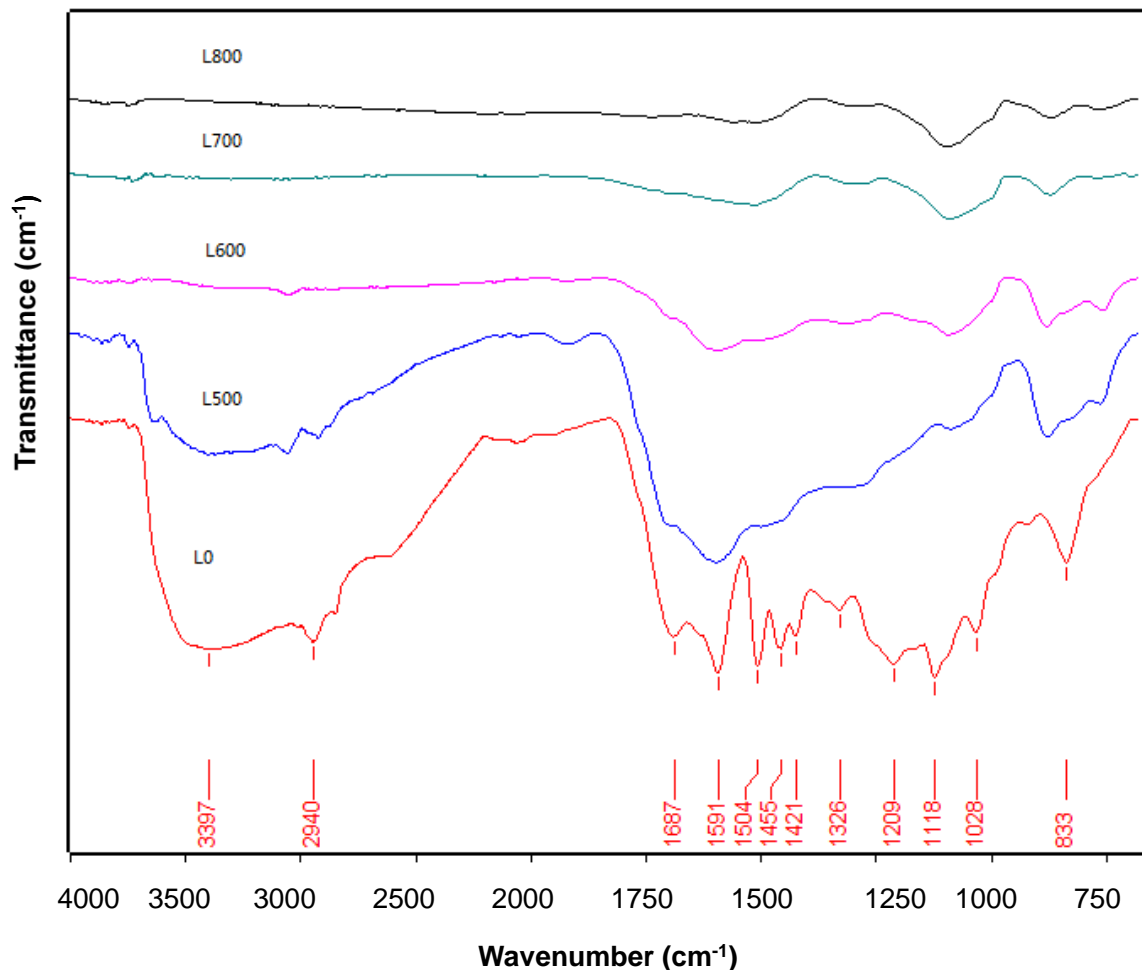


Fig. 3. FTIR spectra of the charcoal obtained from carbonization of lignin at different temperatures

Thermal Stability, Morphology, and Physical Properties

The TGA of the samples is illustrated in Fig. 4. The original lignin sample showed typical degradation curves of lignin. A slight decrease of the mass below 200 °C was observed mainly due to the removal of the residual moisture. The major degradation of lignin that occurred at 200 °C to 500 °C was attributed to the pyrolysis of lignin to produce volatile gases. Correspondingly, a big exothermic peak was observed at 449 °C in the differential thermal analysis (DTA) of L0. After carbonization, the samples showed good thermal stability. At a high temperature of 700 °C, the residual mass of the samples was 82.2%, 92.4%, 96.3%, and 96.6% for L500, L600, L700, and L800, respectively. The TGA illustrated that the charcoal obtained from carbonization at 600 and 800 °C showed good thermal stability where the weight loss was less than 10% when heated at 700 °C. The charcoal product thus obtained was a carbon-rich precursor for the production of activated carbon, which is an absorption material used mainly for waste water and gas treatments as

well as in energy storage (*e.g.*, electrode). Overall, this study provides some fundamental knowledge on the lignin carbonization.

SEM images of the charcoal from carbonization at 800 °C and the pristine lignin are shown in Fig. 5. Clearly, the charcoal had more porous structure and more surface area. In addition, the bulk density of the sample L800 was 0.554 g/cm³, higher than that of the lignin raw material (0.381g/cm³).

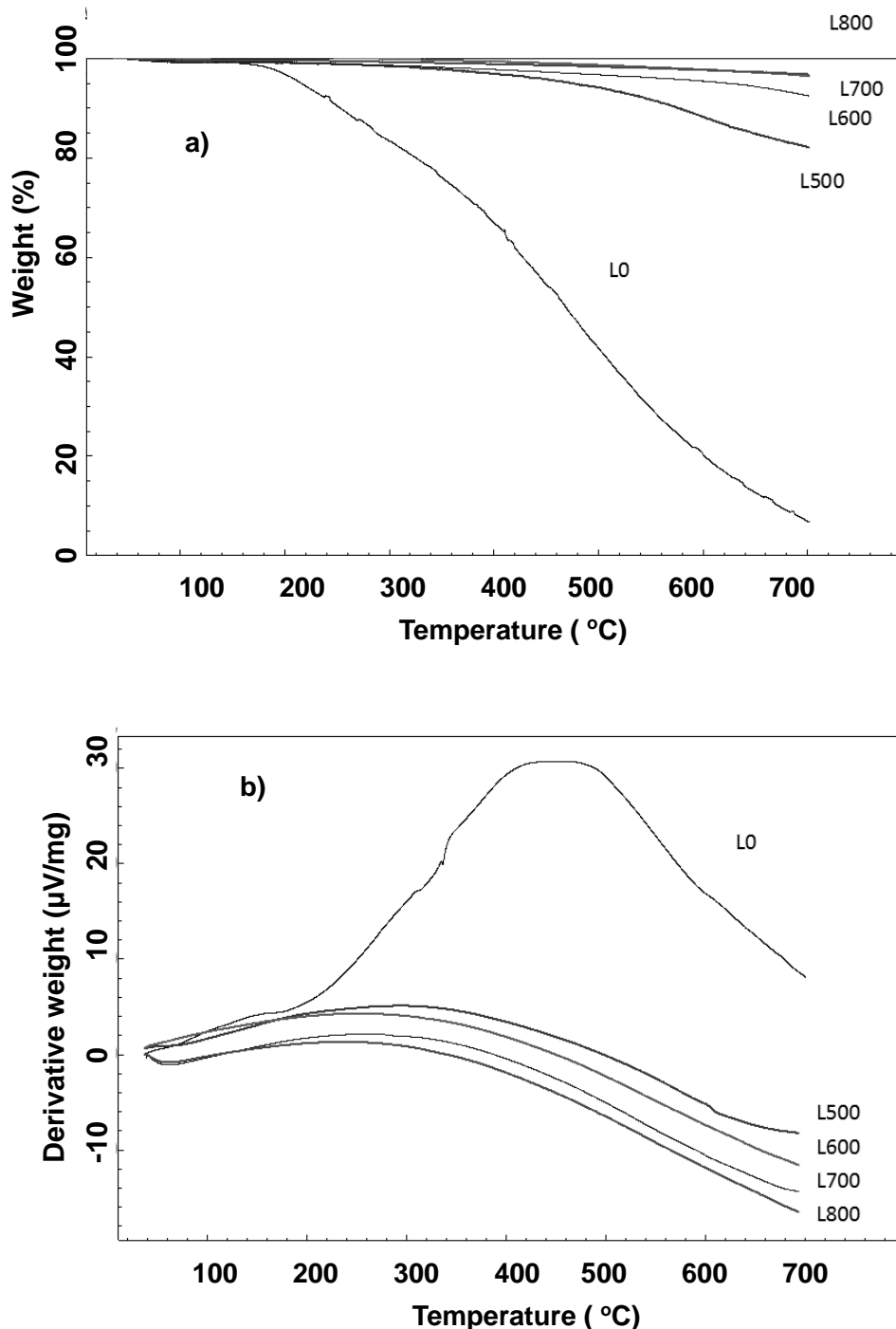


Fig. 4. TGA (a) and DTA (b) curves of the charcoal obtained from carbonization of lignin at different temperatures

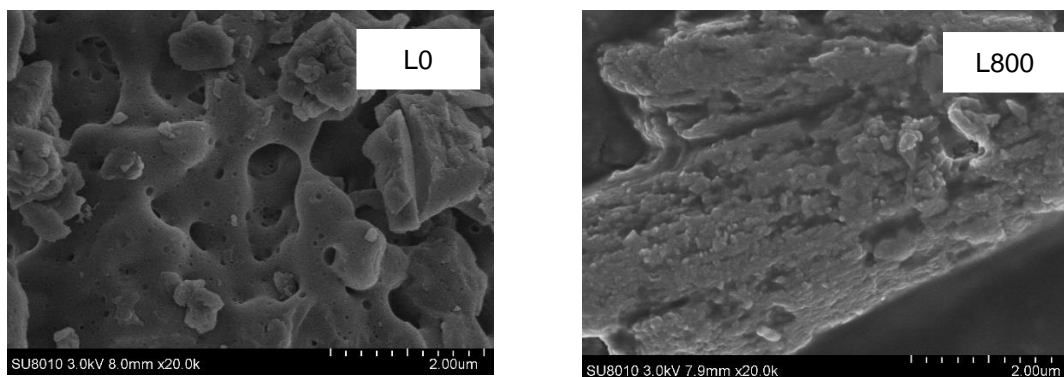


Fig. 5. SEM images of the charcoal obtained from carbonization at 800 °C compared to the unheated lignin

CONCLUSIONS

1. Biorefined lignin was carbonized in a tubular reactor under carbon dioxide atmosphere at 500 °C to 800 °C. As the temperature was increased, the mass yield of lignin decreased due to the removal of volatile components during pyrolysis. The carbonization at higher temperature led to an increment of C-content and decrement in both the H- and O- contents. The charcoal produced from carbonization at 600 and 800 °C showed good thermal stability where the weight loss was less than 10% when heated at 700 °C.
2. An FTIR spectroscopy analysis indicated that the carbonization process resulted in the transformation of phenyl to complex aromatic rings as well as the rearrangement of the aromatic polymers. The study provided some fundamental knowledge on the carbonization of lignin under a carbon dioxide atmosphere as well as its potential application.

ACKNOWLEDGMENTS

This work was financially supported by the Fundamental Research Funds for the Central Universities (2017PT06), National Natural Science Foundation of China (21706014), and Beijing Outstanding Talents Training Project (2016000020124G044).

REFERENCES CITED

- Bilgic, E., Yaman, S., Haykiri-Acma, H., and Kucukbayrak, S. (2016). "Is torrefaction of polysaccharides-rich biomass equivalent to carbonization of lignin-rich biomass?," *Bioresour. Technol.* 200, 201-207. DOI: 10.1016/j.biortech.2015.10.032
- Cao, J., Xiao, G., Xu, X., Shen, D. K., and Jin, B. S. (2013). "Study on carbonization of lignin by TG-FTIR and high-temperature carbonization reactor," *Fuel Process. Technol.* 106, 41-47. DOI: 10.1016/j.fuproc.2012.06.016

- Castro, A. F. N. M., Castro, R. V. O., Carneiro, A. d. C. O., Carvalho, A. M. M. L., da Silva, C. H. F., Cândido, W. L., and dos Santos, R. C. (2017). "Quantification of forestry and carbonization waste," *Renew. Energ.* 103, 432-438. DOI: <http://dx.doi.org/10.1016/j.renene.2016.11.050>
- Correa, C. R., Stollovsky, M., Hehr, T., Rauscher, Y., Rolli, B., and Kruse, A. (2017). "Influence of the carbonization process on activated carbon properties from lignin and lignin-rich biomasses," *ACS Sustain. Chem. Eng.* 5(9), 8222-8233. DOI: 10.1021/acssuschemeng.7b01895
- Correia, R., Gonçalves, M., Nobre, C., and Mendes, B. (2017). "Impact of torrefaction and low-temperature carbonization on the properties of biomass wastes from *Arundo donax* L. and *Phoenix canariensis*," *Bioresour. Technol.* 223, 210-218. DOI: 10.1016/j.biortech.2016.10.046
- Dávila, J. A., Rosenberg, M., Castro, E., and Cardona, C. A. (2017). "A model biorefinery for avocado (*Persea americana* Mill.) processing," *Bioresour. Technol.* 243, 17-29. DOI: 10.1016/j.biortech.2017.06.063
- Demirbas, A. (2009). "Sustainable charcoal production and charcoal briquetting," *Energ. Sour. Part A*, 31(19), 1694-1699. DOI: 10.1080/15567030802094060
- Gao, P., Zhou, Y., Meng, F., Zhang, Y., Liu, Z., Zhang, W., and Xue, G. (2016). "Preparation and characterization of hydrochar from waste eucalyptus bark by hydrothermal carbonization," *Energy*. 97, 238-245. DOI: <http://dx.doi.org/10.1016/j.energy.2015.12.123>
- Hidayat, W., Qi, Y., Jang, J. H., Febrianto, F., Lee, S. H., Chae, H. M., Kondo, T., and Kim, N. H. (2017). "Carbonization characteristics of juvenile woods from some tropical trees planted in Indonesia," *J. Fac. Agr. Kyushu. U.* 62(1), 145-152. DOI: 10.1016/j.biortech.2012.10.148
- Hu, J., Xiao, R., Shen, D., and Zhang, H. (2013). "Structural analysis of lignin residue from black liquor and its thermal performance in thermogravimetric-Fourier transform infrared spectroscopy," *Bioresour. Technol.* 128, 633-639. DOI: 10.1016/j.biortech.2012.10.148
- Ishimaru, K., Hata, T., Bronsveld, P., Meier, D., and Imamura, Y. (2007). "Spectroscopic analysis of carbonization behavior of wood, cellulose and lignin," *J. Mater. Sci.* 42(1), 122-129. DOI: 10.1007/s10853-006-1042-3
- Ismailova, M. G. (2009). "Influence of the carbonization conditions on the formation of the porous structure of activated carbon from cotton lignin," *Prot. Met. Phys. Chem. S.* 45(2), 212-215. DOI: 10.1134/s2070205109020154
- Liu, W. J., Jiang, H., and Yu, H. Q. (2015). "Thermochemical conversion of lignin to functional materials: a review and future directions," *Green Chem.* 17(11), 4888-4907. DOI: 10.1039/c5gc01054c
- Ma, R. S., Guo, M., and Zhang, X. (2014). "Selective conversion of biorefinery lignin into dicarboxylic acids," *ChemSusChem* 7(2), 412-415. DOI: 10.1002/cssc.201300964
- Mudraboyina, B. P., Farag, S., Banerjee, A., Chaouki, J., and Jessop, P. G. (2016). "Supercritical fluid rectification of lignin pyrolysis oil methyl ether (LOME) and its use as a bio-derived aprotic solvent," *Green Chem.* 18(7), 2089-2094. DOI: 10.1039/c5gc02233a
- Pandey, M. P., and Kim, C. S. (2011). "Lignin depolymerization and conversion: a review of thermochemical methods," *Chem. Eng. Technol.* 34(1), 29-41. DOI: 10.1002/ceat.201000270

- Pohlmann, J. G., Osorio, E., Vilela, A. C. F., Diez, M. A., and Borrego, A. G. (2014). "Integrating physicochemical information to follow the transformations of biomass upon torrefaction and low-temperature carbonization," *Fuel* 131, 17-27. DOI: 10.1016/j.fuel.2014.04.067
- Protasio, T. D., Trugilho, P. F., Napoli, A., da Silva, M. G., and Couto, A. M. (2014). "Mass and energy balance of the carbonization of babassu nutshell as affected by temperature," *Pesqui. Agropecu. Bras* 49(3), 189-196. DOI: 10.1590/S0100-204x2014000300005
- Pulido-Novicio, L., Hata, T., Kurimoto, Y., Doi, S., Ishihara, S., and Imamura, Y. (2001). "Adsorption capacities and related characteristics of wood charcoals carbonized using a one-step or two-step process," *J. Wood. Sci.* 47(1), 48-57. DOI: 10.1007/s00226-016-0828-y
- Qi, Y., Jang, J. H., Hidayat, W., Lee, A. H., Lee, S. H., Chae, H. M., and Kim, N. H. (2016). "Carbonization of reaction wood from *Paulownia tomentosa* and *Pinus densiflora* branch woods," *Wood Sci. Technol.* 50(5), 973-987. DOI: 10.1007/s00226-016-0828-y
- Ronsse, F., Nachenius, R. W., and Prins, W. (2015). "Carbonization of biomass," 293-324. DOI: 10.1016/b978-0-444-63289-0.00011-9
- Sahoo, S., Seydibeyoglu, M. O., Mohanty, A. K., and Misra, M. (2011). "Characterization of industrial lignins for their utilization in future value added applications," *Biomass Bioenerg.* 35(10), 4230-4237. DOI: 10.1016/j.biombioe.2011.07.009
- Savova, D., Apak, E. C., Ekinci, E., Yardim, F., Petrov, N., Budinova, T., Razvigorova, M., and Minkova, V. (2001). "Biomass conversion to carbon adsorbents and gas," *Biomass. Bioenerg.* 21(2), 133-142. DOI: 10.1016/j.biombioe.2011.07.009
- Souto, F., Calado, V., and Pereira, N. (2015). "Carbon fiber from lignin: A literature review," *Materia-Rio De Janeiro* 20(1), 100-114. DOI: 10.1590/s1517-707620150001.0012
- Suhas, Carrott, P. J. M., and Carrott, M. M. L. R. (2007). "Lignin from natural adsorbent to activated carbon: A review," *Bioresour. Technol.* 98(12), 2301-2312. DOI: 10.1016/j.biortech.2006.08.008
- Suzuki, T., Yamada, T., Okazaki, N., Tada, A., Nakanishi, M., Futamata, M., and Chen, H.-T. (2001). "Electromagnetic shielding capacity of wood char loaded with nickel," *Mater. Sci. Res. Int.* 7(3), 206-212.
- Wikberg, H., Ohra-aho, T., Pileidis, F., and Titirici, M.-M. (2015). "Structural and morphological changes in kraft lignin during hydrothermal carbonization," *ACS Sustain. Chem. Eng.* 3(11), 2737-2745. DOI: 10.1021/acssuschemeng.5b00925
- Zhao, X. B., and Zhu, J. Y. (2016). "Efficient conversion of lignin to electricity using a novel direct biomass fuel cell mediated by polyoxometalates at low temperatures," *ChemSusChem* 9(2), 197-207. DOI: 10.1002/cssc.201501446

Article submitted: February 26, 2018; Peer review completed: July 7, 2018; Revised version received: July 16, 2018; Accepted: July 17, 2018; Published: July 19, 2018. DOI: 10.15376/biores.13.3.6736-6745